IEICE TRANS. COMMUN., VOL.E103–B, NO.11 NOVEMBER 2020

INVITED PAPER *Joint Special Section on Opto-electronics and Communications for Future Optical Network*

Available Spectral Space in C-Band Expansion Remaining After Optical Quantization Based on Intensity-to-Lambda Conversion

Yuta KAIHORI[†a)], ***Nonmember***, **Yu YAMASAKI**[†], ***Student Member***, ***and*** **Tsuyoshi KONISHI**[†], ***Member***

SUMMARY A high degree of freedom in spectral domain allows us to accommodate additional optical signal processing for wavelength division multiplexing in photonic analog-to-digital conversion. We experimentally verified a spectral compression to save a necessary bandwidth for soliton self-frequency shift based optical quantization through the cascade of the four-wave mixing based and the sum-frequency generation based spectral compression. This approach can realize 0.03 nm individual bandwidth correspond to save up to more than 85 percent of bandwidth for 7-bit optical quantization in C-band.

key words: *photonic analog-to-digital conversion, optical quantization, spectral compression, four-wave mixing, sum-frequency generation*

1. Introduction

The use of an advanced high bit rate optical signal such as a quadrature amplitude modulation optical signal places more load on both the transceiver and receiver sides. At the front end of the receiver side, such a situation makes it necessary to upgrade the bit-rate performance of analog-to-digital conversion (ADC) by introducing optical signal processing starting with optical sampling [1]. ADC is basically composed of sampling, quantization, and coding, and optical technology has already been introduced and installed in the sampling part of some commercial oscilloscopes [2]. Also, 7-bit 40 GSps with optical sampling and interleaving has been reported [3]. While optical signal processing in the sampling part overcomes the sampling rate limitation of electrical sampling due to its timing jitter issue, the acceleration of the sampling rate requires a high degree of parallelism of subsequent low-speed quantization and coding parts to match their narrow bandwidth with that of the preceding high-speed sampling part. Since a higher degree of parallelism requires a higher power consumption, optical quantization and coding are expected to solve the power consumption issue by minimizing the degree of parallelism, and several approaches have been investigated in this regard [4]–[10]. Optical intensity-to-lambda conversion can achieve optical quantization with a single architecture based on wavelength division multiplexing (WDM), and soliton self-frequency shift (SSFS)-based optical quantization has been proposed and investigated as one of the promising approaches [4]–[7]. Since SSFS is one of the ultrafast nonlinear effects in a fiber, it can certainly satisfy the bandwidth matching with high-speed optical sampling over several tens of GSps. In fact, 3.8-bit 40 GSps optical sampling and quantization have been demonstrated [5]. However, since it requires a broad lambda region for improving its resolution over 7-bit, overextension of the lambda region beyond the C-band (1530–1565 nm) in order to accommodate such broadband signals induces additional costs regarding power consumption and complexity. Recently, we successfully demonstrated 0.2 nm bandwidth spectral compression using four-wave mixing (FWM) in a communication band which could realize over 7-bit optical quantization based on intensity-to-lambda conversion within 35 nm-bandwidth of C-band [11]. To accommodate additional optical signal processing for WDM technology, it is attractive to provide a high degree of freedom in wavelength domain by further spectral compression. However, generation of the third order nonlinear effects is suitable for a short pulse signal with a broad bandwidth but not for a spectral compressed signal with a relatively narrow bandwidth. On the other hand, a periodically poled lithium niobate (PPLN) waveguide has a potential to provide the highly efficient second order nonlinear effect for light a relatively narrow bandwidth.

In this work, we introduce sum-frequency generation (SFG)-based spectral compression [13], [14] using a PPLN waveguide and realize a further spectral compression to save a necessary bandwidth for optical quantization. The experimental results show a necessary bandwidth less than 4 nm after SFG-based spectral compression, which could realize over 7-bit optical quantization based on intensity-to-lambda conversion.

2. Technical Background and Method

Figure 1 shows the schematic diagram of the SSFS-based optical quantization.

An optically sampled signal induces SSFS when propagating in a high-nonlinear fiber (HNLF) and its center wavelength shifts to a longer wavelength, which is approximately proportional to the peak power (analog level) of each optically sampled signal (intensity-to-lambda conversion). Each SSFS signal is identified by a WDM de-multiplexing (DeMUX) device like an arrayed waveguide grating (AWG) for quantization and is separated into different ports according to each analog level. Each output port can provide a level identification signal for subsequent coding. The number of bits (NOB), namely the resolution of the SSFS-based optical

Manuscript received December 20, 2019.
Manuscript revised March 26, 2020.
Manuscript publicized May 14, 2020.

[†]The authors are with Graduate School of Engineering, Osaka University, Suita-shi, 565-0871 Japan.
a) E-mail: kaihori@photonics.mls.eng.osaka-u.ac.jp

DOI: 10.1587/transcom.2019OBI0002

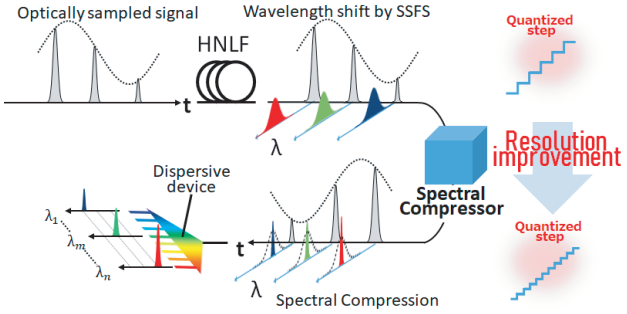

Fig. 1 Schematic diagram of SSFS-based optical quantization.

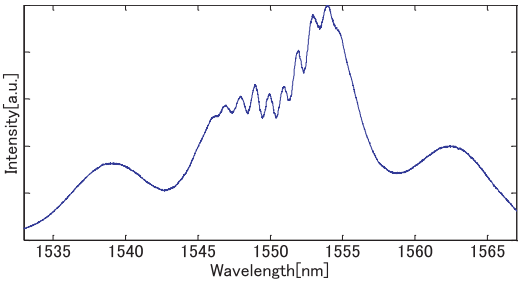

Fig. 2 The spectrum of the light source (Calmar FPL-M2CFF-OSU-01).

quantization is given by

$$\mathrm{NOB} = \log_2\left(\frac{\lambda_{shift} + \Delta\lambda_{FWHM}}{\Delta\lambda_{FWHM}}\right), \tag{1}$$

where λ_{shift} and $\Delta\lambda_{FWHM}$ are the amount of center wavelength shift and the bandwidth of the optically sampled signal after SSFS, respectively. Equation (1) shows that the resolution can be improved by increasing λ_{shift} and decreasing $\Delta\lambda_{FWHM}$. The increment of λ_{shift} and the decrement of $\Delta\lambda_{FWHM}$ are experimentally demonstrated using the chirped-pulse amplification technique [6] and the self-phase modulation (SPM)-based spectral compression [7]–[10], [12], respectively. However, as mentioned, taking the additional cost due to the overextension of the lambda region into consideration, the increment of λ_{shift} should be limited within the C-band; hence, we focused on decreasing $\Delta\lambda_{FWHM}$ for improving the resolution over 7-bit. Since the SPM cannot function properly after a certain degree of spectral compression, it is necessary to examine different spectral compression approaches that can work regardless of the degree of spectral compression. Possible approaches include FWM-based and SFG-based ones.

FWM-based spectral compression can be realized by the degenerate four-wave mixing of two linearly chirped pulses and it is suitable for optical pulses with relatively broad bandwidth. Degenerate FWM is one of the third-order nonlinear optical effects used for ultrafast signal processing. Degenerate FWM provides idler waves of frequency $2f_1 - f_2$ and $2f_2 - f_1$ from input waves of frequency f_1 and f_2. Here, when degenerate FWM is induced by the two linearly chirped pulses, which have instantaneous frequencies of $f_1(t) = f_1 + at$ and $f_2(t) = f_2 + 2at$, the instantaneous frequencies of the pulses generated from the degenerate FWM are given by

$$\begin{aligned} 2f_1(t) - f_2(t) &= 2(f_1 + at) - (f_2 + 2at) \\ &= 2f_1 - f_2, \\ 2f_2(t) - f_1(t) &= 2(f_2 + 2at) - (f_1 + at) \\ &= 2f_2 - f_1 + 3at, \end{aligned} \tag{2}$$

where a and t are the amount of linear chirp and the temporal position in the case that the center of temporal waveform is 0 [s], respectively. From Eq. (2), it can be seen that degenerate FWM can ideally compress the bandwidth of a linearly chirped broadband signal into that of a single wavelength signal having a center frequency of $2f_1 - f_2$.

SFG-based spectral compression can be realized by the second order nonlinear optical effect [13], [14] and a PPLN waveguide has a potential to provide the highly SFG efficiency for light a relatively narrow bandwidth [15]–[18]. SFG provides the waves of frequency $f_1 + f_2$ from input waves of frequency f_1 and f_2. Then, when SFG is induced by two chirped pulses which have instantaneous frequencies $f_1(t) = f_1 + at$ and $f_2(t) = f_2 - at$, the instantaneous frequencies of the pulses generated from the SFG are given by

$$f_1(t) + f_2(t) = f_1 + f_2 + at - at = f_1 + f_2, \tag{3}$$

From Eq. (3), it can be seen that SFG can achieve spectral compression same as FWM-based spectral compression.

3. Experiment

We experimentally verified FWM-based spectral compression and SFG-based spectral compression.

3.1 FWM-Based Spectral Compression

Figure 3 shows the experimental setup for verifying the FWM-based spectral compression in a communication band. We used optical pulses irradiated from a fiber laser (Calmar FPL-M2CFF-OSU-01) as the light source for demonstrating spectral compression. The pulse width and repetition rate were 100 fs, and 30 MHz, respectively. Its spectrum is shown in Fig. 2.

By means of the wavelength selective switch (WSS), pulses having center wavelengths of 1546 nm and 1552 nm were output from port 1 and port 2, respectively. The bandwidths of the pulses from port 1 and port 2 were 3 nm and 5 nm, respectively. The pulse from port 1 was propagated through 600 m HNLF (D = 4.78 [ps/nm/km], S = 0.022 [ps^2/nm/km], γ = 11 [/W/km]) for the generation of SSFS. The band-pass filter (BPF) passed only the wavelength shifted signal. In order to provide a linear chirp to the pulse, it was propagated through 500 m single-mode fiber (SMF). The pulse from port 2 was provided a chromatic dispersion of 17 [ps/nm] by the WSS. They were multiplexed by the 3 dB coupler and were propagated through 92 m HNLF (D = −0.0185 [ps/nm/km], S = 0.03 [ps^2/nm/km], γ = 16 [/W/km]) for generating the FWM. In order to

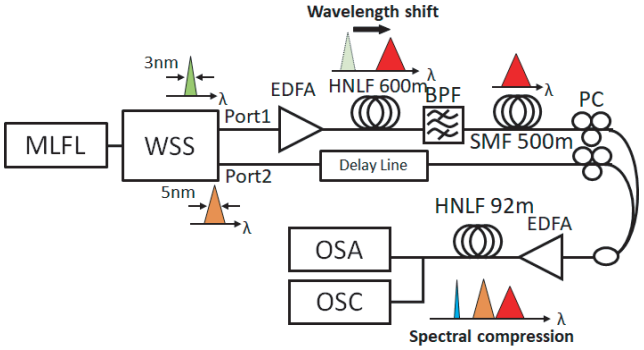

Fig. 3 Experimental setup of FWM-based spectral compression for the signal after SSFS: MLFL (mode-locked fiber laser), WSS (wavelength selective switch), HNLF (high-nonlinear fiber), EDFA (erbium-doped fiber amplifier), BPF (band-pass filter), SMF (single-mode fiber), PC (polarization controller), OSA (optical spectrum analyzer), OSC (oscilloscope).

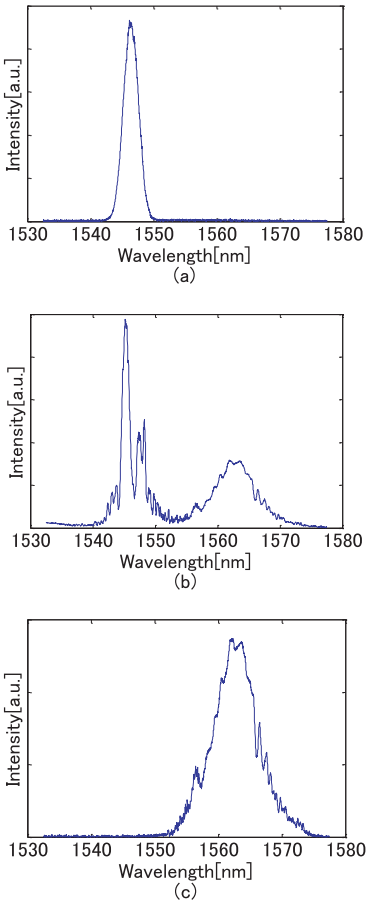

Fig. 4 Experimental results of the spectra (a) before and (b) after inducing SSFS, and (c) of the signal filtered by BPF on the right side of the spectrum (b).

match the input timing of the pulses from port 1 and port 2 to HNLF, we used the optical delay line.

Figures 4(a) and (b) show the input and output spectra of the 600 m HNLF for generating SSFS. Fig. 4(c) shows the signal filtered by the BPF.

Figures 5(a) and (b) show the input and output spectra of the 92 m HNLF for generating degenerate FWM. Figure 5(c) shows the spectrum of the idler wave. As shown in Figs. 5(b) and (c), the narrowband signal is generated near 1543 nm. Its bandwidth is approximately 0.2 nm. From these results, we can confirm FWM-based spectral compression for the signal after SSFS.

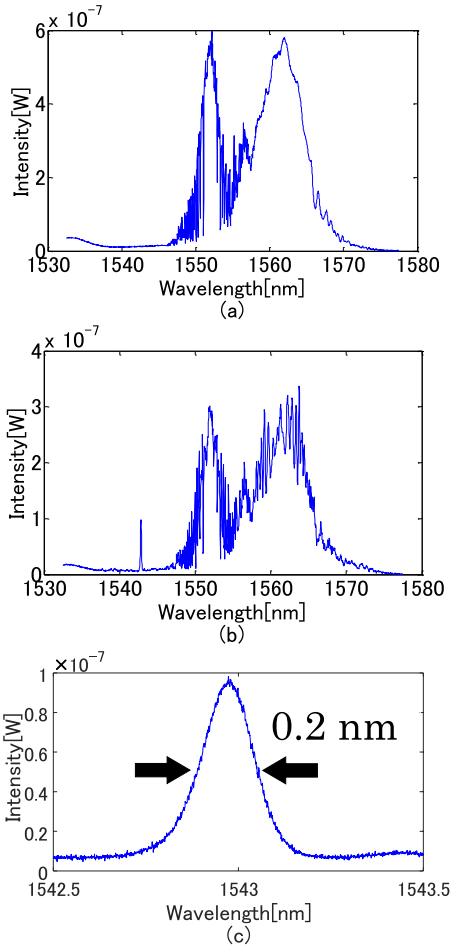

Fig. 5 Experimental results of the spectra (a) before and (b) after inducing FWM-based spectral compression (c) enlarging the compressed idler signal around 1543 nm of the spectrum (b).

As preparation for introducing FWM-based spectral compression to optical quantization, we experimentally demonstrated this spectral compression in the signals which have the different center wavelength.

Figure 6 shows the experimental setup for verifying the FWM-based spectral compression for the signals which have the different center wavelength. By means of the WSS, the pulses which have the center wavelength 1556 nm, 1556.5 nm, 1557 nm, 1557.5 nm, 1558 nm were output from port 1 and the pulse which has center wavelength 1550 nm was output from port 2. The bandwidth of these pulses were 5 nm. These pulses were provided chromatic dispersion and generated FWM in the same way.

Figure 7 shows the FWM-based spectral compression results of different lambda signals. As shown in Fig. 7, it can be seen that the spectral intensity of the light source de-

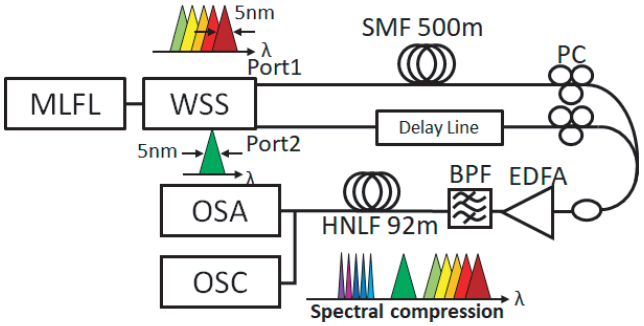

Fig. 6 Experimental setup of FWM-based spectral compression for the different lambda signals. MLFL (mode-locked fiber laser), WSS (wavelength selective switch), HNLF (high-nonlinear fiber), EDFA (erbium-doped fiber amplifier), BPF (band-pass filter), SMF (single-mode fiber), PC (polarization controller), OSA (optical spectrum analyzer), OSC (oscilloscope).

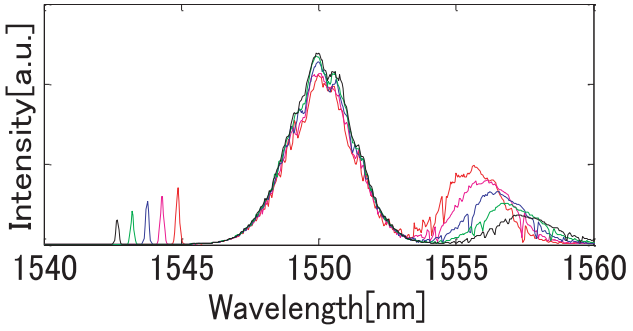

Fig. 7 FWM-based spectral compression results of changing the center wavelength from 1556 nm to 1558 nm by 0.5 nm. The groups of spectra around 1557 nm and 1543 nm are the output signals from WSS port 1 and the compressed idler signals, respectively.

creases after 1556 nm as shown in Fig. 2, therefore, as the center wavelength of the pulse is increased beyond 1556 nm, its intensity decreases. From these results, we can confirm that the center wavelength of each idler signal can properly change in response to those of the input signals while retaining the amount of wavelength shift required for optical quantization.

3.2 SFG-Based Spectral Compression

Figure 8 shows the experimental setup for verifying the SFG-based spectral compression. In this experiment, in order to prevent from increasing the complexity, we used mm order PPLN waveguide which is common size of PPLN waveguide as the SFG device [15]–[17]. We used the optical source same as Sect. 3.1. By means of the WSS, pulses having center wavelengths of 1546 nm, 1550 nm and 1550 nm were output from port 1, port 2, and port 3 respectively. The bandwidths of the pulses from port 1, port 2 and port 3 were 3 nm, 5 nm, and 0.2 nm respectively. First, the SSFS signal was generated and compressed by FWM-based spectral compression in the same way as Sect. 3.1. In this experiment, in order to improve the conversion efficiency, we improved the nonlinearity by using HNLF longer

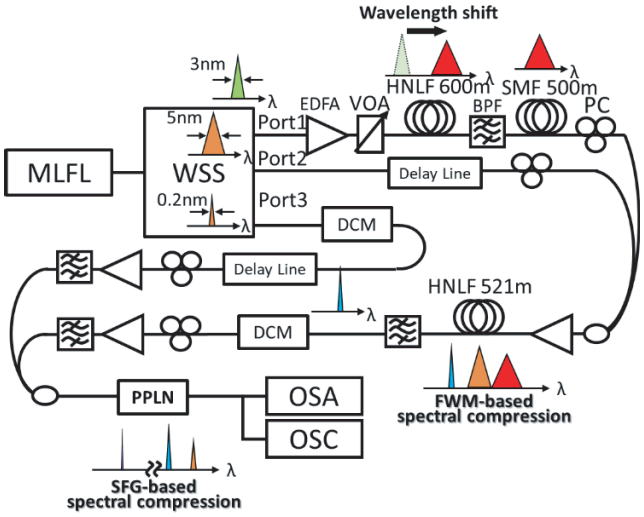

Fig. 8 Experimental setup of SFG-based spectral compression for the signal after SSFS: MLFL (mode-locked fiber laser), WSS (wavelength selective switch), HNLF (high-nonlinear fiber), EDFA (erbium-doped fiber amplifier), VOA (variable optical attenuator), BPF (band-pass filter), SMF (single-mode fiber), PC (polarization controller), DCM (dispersion compensation module), PPLN (periodically poled lithium niobate), OSA (optical spectrum analyzer), OSC (oscilloscope).

than used in Sect. 3.1. The pulses from port 1 and 2 were propagated through 521 m HNLF (D = 0.055 [ps/nm/km], S = 0.029 [ps^2/nm/km], γ = 16 [/W/km]) for generating the FWM. We postulated the future use of silicon nanowire by using the higher nonlinearity device for improvement of the FWM conversion efficiency [19]. Silicon waveguide has been investigated and expected to be one of the promising integration approaches because it has several tens thousand higher nonlinear coefficient γ than conventional HNLF [20]. The BPF after 521 m HNLF passed only the idler. The idler and the signal from port 3 were provided chromatic dispersion −500 [ps/nm] and 500 [ps/nm] respectively by the dispersion compensation modules (TeraXion TDCMX). The BPF after erbium-doped fiber amplifier removed amplified spontaneous emission noise. They were multiplexed by 3 dB coupler and propagated to PPLN ridge waveguide (Z-cut, conversion efficiency ∼0.037% when continuous wave lights at 1550 nm and 1542 nm with 0.5 mW are converted to 773 nm) for generating SFG. As with inducing FWM, in order to match the input timing of the two pulses to PPLN, we used the optical delay line.

Figures 9(a) and (b) show the input and output spectra of the 600 m HNLF for generating SSFS. Fig. 9(c) shows the signal filtered by the BPF after 600 m HNLF.

Figures 10(a) and (b) show the experimental result of FWM-based spectral compression for SSFS signal. The narrowband signal is generated near 1542 nm.

As shown in Fig. 10(b), the compressed signal was generated more strongly than Fig. 5(b), the experimental result by using 92 m HNLF. From this result, high nonlinearity devices are expected to improve FWM-based spectral compression for optical quantization.

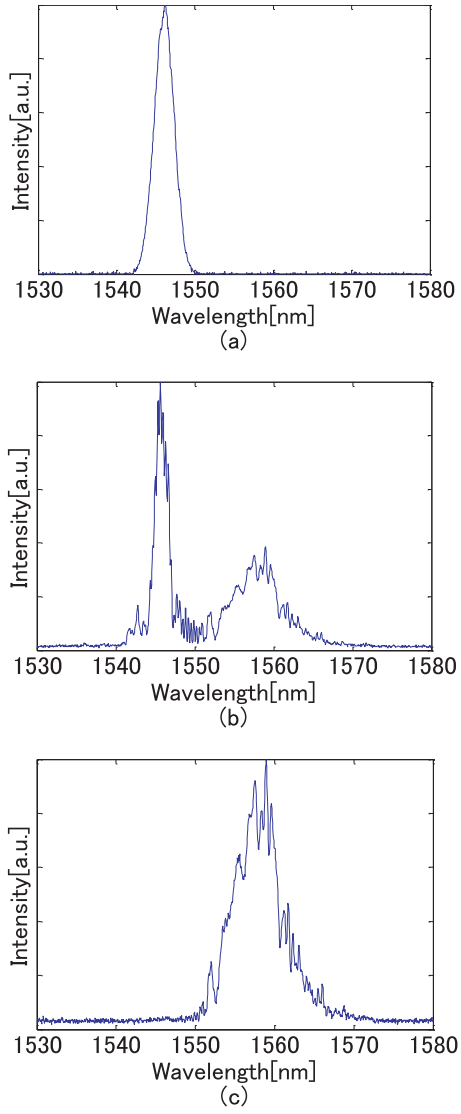

Fig. 9 Experimental results of the spectra (a) before and (b) after inducing SSFS, and (c) of the signal filtered by BPF after 600 m HNLF.

Figures 11(a) and (b) show the spectra of input and output PPLN, respectively. In Fig. 11(a), the intensity of the signal of 1550 nm from port 3 was very low because the light source was divided into three ports of WSS. As shown in Fig. 11(b), the bandwidth of the SFG signal is remarkably narrower than the compressed bandwidth of 0.2 nm by FWM-based spectral compression and the obtained bandwidth is approximately 0.03 nm. From these results, we successfully confirmed the further spectral compression for a SSFS signal through the cascade of the FWM-based and SFG-based spectral compression.

In order to verify the applicability of SFG-based spectral compression for SSFS-based optical quantization, we examined the input power dependencies of the center wavelength after the cascade of the SSFS, the FWM-based, and SFG-based spectral compression. Fig. 12 shows the spectra after FWM-based spectral compression for the different

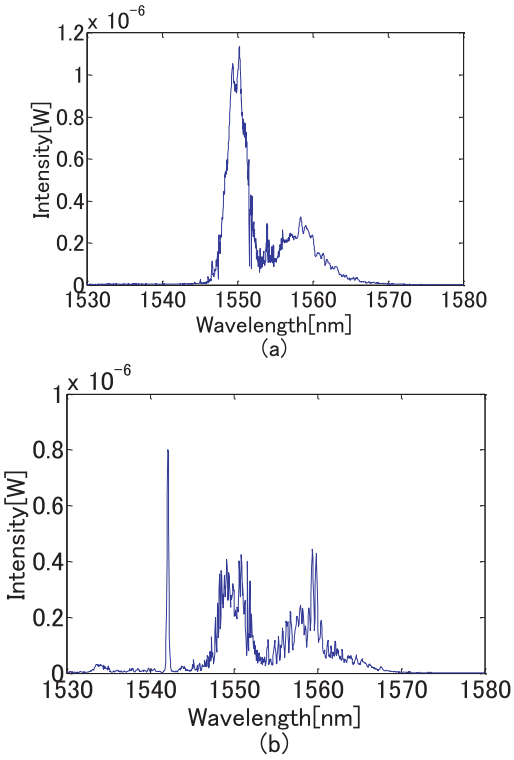

Fig. 10 Experimental results of the spectra (a) before and (b) after FWM-based spectral compression. The narrowband signal near 1542 nm is the compressed idler signal.

lambda SSFS signals corresponding to the different input power. From Fig. 12, it can be seen that both of the center wavelength of the SSFS signals and the compressed idler signals were interlockingly shifted depending on the input power.

Figures 13(a) and (b) show the experimental results of spectra before and after the further spectral compression through SFG-based spectral compression for the different lambda SSFS signals after FWM-based spectral compression corresponding to the different input power. From Fig. 13(a), the bandwidths of idler signals are less than 0.4 nm before SFG-based spectral compression and they are within the allowable range of the PPLN used in this experiment. From Fig. 13(b), the bandwidths of SFG signals are less than 0.03 nm after SFG-based spectral compression. From these results, we confirmed that each of the input PPLN signals were properly compressed.

As mentioned before, the length of PPLN waveguide is about several mm. Therefore, SFG-spectral compression is expected to be achieved by a compact system and not to bring about increase of the complexity. Moreover, the optical components such as couplers, polarization control devices, etc and AWG for De-MUX of the compressed signals have been demonstrated on silicon [21], [22]. They are expected to be integrated by silicon photonics technology.

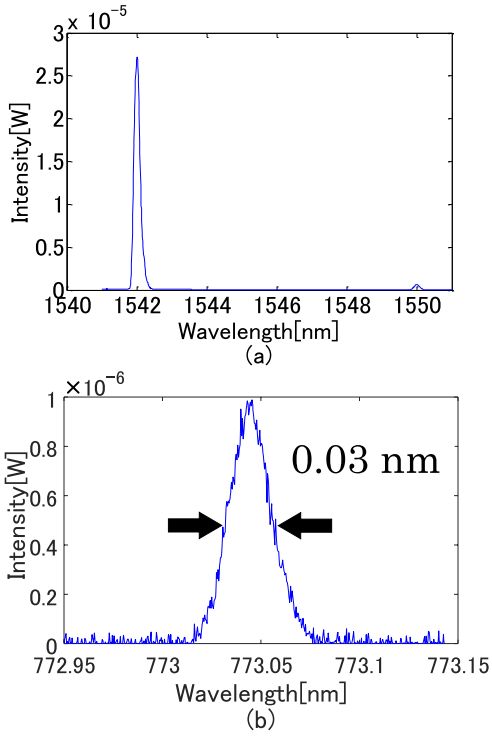

Fig. 11 Experimental results of the spectra of (a) input and (b) output of PPLN. The signal of center wavelength 1542 nm and 1550 nm are the compressed idler signal by FWM-based spectral compression and the signal output from WSS port 3, respectively.

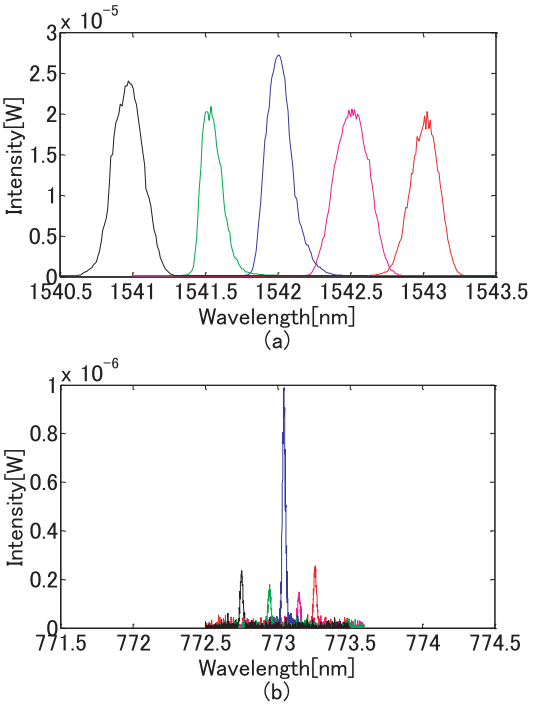

Fig. 13 Experimental results of spectra (a) before and (b) after further spectral compression through SFG-based spectral compression for different lambda SSFS signals after FWM-based spectral compression corresponding to the different input power signals.

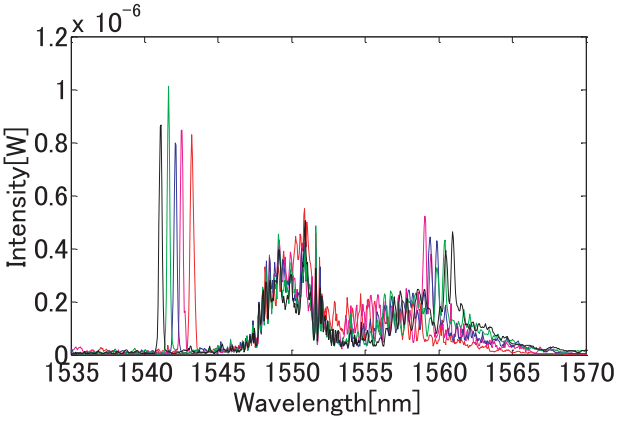

Fig. 12 Spectra after FWM-based spectral compression for different lambda SSFS signals corresponding to different input power which is changed by variable optical attenuator (VOA). The groups of spectra around 1560 nm and 1543 nm are those of SSFS signals and idler signals after FWM-based spectral compression, respectively.

4. Discussion

A nanophotonic PPLN waveguide is reported to show a very broad bandwidth performance (~10 nm at C-band) [15], but there is a tendency that conventional PPLNs have a narrow bandwidth performance (~1 nm at C-band) and the generated SFG-efficiency strongly depends on the wavelengths of input lights [16]–[18]. The PPLN used in this experiment has the relatively narrow bandwidth of 2 nm at C-band and it is optimally designed for the output light wavelength of 773 nm from the input light wavelengths of 1550 nm and 1542 nm. In fact, the output power is highest near 773 nm, as shown in Fig. 12.

Here, we discuss the degree of bandwidth saving to provide a design guideline of appropriate individual compressed bandwidth to satisfy the demand of the NOB. Figure 14 shows the necessary bandwidth for optical quantization as a function of the individual compressed bandwidth for different values of the NOB. A necessary bandwidth is determined so as to satisfy the demand of the compressed bandwidth and the NOB. We estimated the necessary bandwidth for the compressed signals after re-converted to C-band by wavelength conversion such as difference frequency generation [18], [23]. As shown in Fig. 11(b), the compressed signal of 0.03 nm at 750 nm-band is obtained in experiment. Therefore, by re-conversion of the compressed signals to C-band, the necessary bandwidth for this optical quantization is expected to be significantly reduced by setting the amount of SSFS wavelength shift to smaller. In the case that the PPLN waveguide which has 10 nm bandwidth performance, mentioned in the beginning of this section, is used for this optical quantization, from Eq. (1), the experimental result of 0.03 nm bandwidth after SFG-based spectral compression could realize 8.38-bit optical quantization based on the intensity-to-lambda conversion within one-third of the C-band bandwidth (35 nm). The yellow star mark and the red dotted line in Fig. 14 shows the compressed

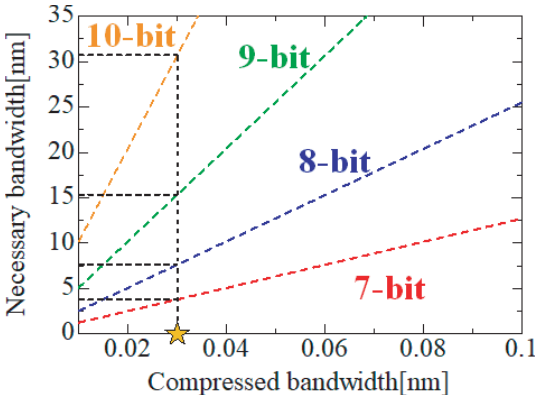

Fig. 14 Necessary bandwidth for optical quantization as a function of the individual compressed bandwidth for different values of the number of bit. The yellow star mark shows compressed bandwidth result of 0.03 nm in this experiment.

bandwidth result of 0.03 nm in this experiment and the necessary bandwidth for 7-bit resolution, respectively. From Fig. 14 it can be said that necessary bandwidth for 7-bit resolution is within the range of less than 4 nm. With the compressed bandwidth result of 0.03 nm, it is expected to be able to save up to more than 85 percent of bandwidth in the C-band for 7-bit resolution and save a high degree of freedom in wavelength domain.

5. Conclusion

We succeeded in a further spectral compression to save a necessary bandwidth for optical quantization through the cascade of the FWM-based and the SFG-based spectral compression. The experimental results show a necessary bandwidth for optical quantization for 7-bit resolution can be compressed to less than 4 nm which is expected to be able to save up to more than 85 percent of bandwidth in the C-band. The achieved bandwidth saving performance is expected to provide a high degree of freedom in wavelength domain so as to accommodate additional optical signal processing based on WDM technology in photonic ADC.

While a PPLN is suitable for integration, a HNLF is still used for spectral compression. The future development of the system comes to require finding out components which can be highly integrated and silicon photonics is expected to be one of promising approaches to satisfy those requirements.

Acknowledgments

This work is partially supported by Mitsubishi Electric Corporation.

References

[1] G.C. Valley, "Photonic analog-to-digital converters," Opt. Express, vol.15, no.5, pp.1955–1982, March 2007.
[2] F. Krausz and M.I. Stockman, "Attosecond metrology: From electron capture to future signal processing," Nature Photonics, vol.8, no.3, pp.205–213, Feb. 2014.
[3] A. Khilo, S.J. Spector, M.E. Grein, A.H. Nejadmalayeri, C.W. Holzwarth, M.Y. Sander, M.S. Dahlem, M.Y. Peng, M.W. Geis, N.A. DiLello, J.U. Yoon, A. Motamedi, J.S. Orcutt, J.P. Wang, C.M. Sorace-Agaskar, M.A. Popović, J. Sun, G. Zhou, H. Byun, J. Chen, J.L. Hoyt, H.I. Smith, R.J. Ram, M. Perrott, T.M. Lyszczarz, E.P. Ippen, and F.X. Kärtner, "Photonic ADC: Overcoming the bottleneck of electronic jitter," Opt. Express, vol.20, no.4, pp.4454–4469, Feb. 2012.
[4] T. Konishi, K. Tanimura, K. Asano, Y. Oshita, and Y. Ichioka, "All-optical analog-to-digital converter by use of self-frequency shifting in fiber and a pulse-shaping technique," J. Opt. Soc. Am. B, vol.19, no.11, pp.2817–2823, Nov. 2002.
[5] T. Nagashima, M. Hasegawa, and T. Konishi. "40 GSample/s all-optical analog to digital conversion with resolution degradation prevention," IEEE Photon. Technol. Lett., vol.29, no.1, pp.74–77, Jan. 2017.
[6] K. Takahashi, H. Matsui, T. Nagashima, and T. Konishi, "Resolution upgrade toward 6-bit optical quantization using power-to-wavelength conversion for photonic analog-to-digital conversion," Opt. Lett., vol.38, no.22, pp.4864–4867, Nov. 2013.
[7] T. Nishitani, T. Konishi, and K. Itoh, "Resolution improvement of all-optical analog-to-digital conversion employing self-frequency shift and self-phase-modulation-induced spectral compression," IEEE J. Sel. Topics Quantum Electron., vol.14, no.3, pp.724–732, June 2008.
[8] T. Nishitani, T. Konishi, and K. Itoh, "Optical coding scheme using optical interconnection for high sampling rate and high resolution photonic analog-to-digital conversion," Opt. Express, vol.15, no.24, pp.15812–15817, Nov. 2007.
[9] T. Konishi, K. Takahashi, H. Matsui, T. Satoh, and K. Itoh, "Five-bit parallel operation of optical quantization and coding for photonic analog-to-digital conversion," Opt. Express, vol.19, no.17, pp.16106–16114, Aug. 2011.
[10] T. Satoh, K. Takahashi, H. Matsui, K. Itoh, and T. Konishi, "10-GS/s 5-bit real-time optical quantization for photonic analog-to-digital conversion," IEEE Photon. Technol. Lett., vol.24, no.10, pp.830–832, May 2012.
[11] Y. Kaihori, Y. Yamasaki, and T. Konishi, "Resolution maximization toward over 7 bit optical quantization based on intensity-to-lambda conversion within C-band," OECC/PSC2019, WF2-2, Fukuoka, Japan, July 2019.
[12] B.R. Washburn, J.A. Buck, and S.E. Ralph, "Transform-limited spectral compression due to self-phase modulation in fibers," Opt. Lett., vol.25, no.7, pp.445–447, April 2007.
[13] F. Raoult, A.C.L. Boscheron, D. Husson, C. Sauteret, A. Modena, V. Malka, F. Dorchies, and A. Migus, "Efficient generation of narrow-bandwidth picosecond pulses by frequency doubling of femtosecond chirped pulses," Opt. Lett., vol.23, no.14, pp.1117–1119, July 1998.
[14] M. Nejbauer, T.M. Kardaś, Y. Stepanenko, and C. Radzewicz, "Spectral compression of femtosecond pulses using chirped volume Bragg gratings," Opt. Lett., vol.41, no.11, pp.2394–2397, May 2016.
[15] C. Wang, C. Langrock, A. Marandi, M. Jankowski, M. Zhang, B. Desiatov, M.M. Fejer, and M. Lončar, "Ultrahigh-efficiency wavelength conversion in nanophotonic periodically poled lithium niobate waveguides," Optica, vol.5, no.11, pp.1438–1441, Nov. 2018.
[16] R. Geiss, S. Saravi, A. Sergeyev, S. Diziain, F. Setzpfandt, F. Schrempel, R. Grange, E. Kley, A. Tünnermann, and T. Pertsch, "Fabrication of nanoscale lithium niobate waveguides for second-harmonic generation," Opt. Lett., vol.40, no.12, pp.2715–2718, June 2015.
[17] S. Carbajo, J. Schulte, X. Wu, K. Ravi, D.N. Schimpf, and F.X. Kärtner, "Efficient narrowband terahertz generation in cryogenically cooled periodically poled lithium niobate," Opt. Lett., vol.40, no.24, pp.5762–5765, Dec. 2015.
[18] C. Langrock, S. Kumar, J.E. McGeehan, A.E. Willner, and M.M. Fejer, "All-optical signal processing using $\chi^{(2)}$ nonlinearities in guided-

wave devices," J. Lightwave Technol., vol.24, no.7, pp.2579–2592, July 2006.
[19] T. Konishi, Y. Kaihori, and Y. Yamasaki, "Power efficient fine spectral compression for high resolution optical quantization based on intensity-to-lambda conversion," 2019 21st International Conference on Transparent Optical Networks (ICTON), Sa.B1.4, Angers, France, July 2019.
[20] J. Leuthold, C. Koos, and W. Freude, "Nonlinear silicon photonics," Nature Photonics, vol.4, no.8, pp.535–544, July 2010.
[21] T. Komljenovic, M. Davenport, J. Hulme, A.Y. Liu, C.T. Santis, A. Spott, S. Srinivasan, E.J. Stanton, C. Zhang, and J.E. Bowers, "Heterogeneous silicon photonic integrated circuits," J. Lightwave Technol., vol.34, no.1, pp.20–35, Jan. 2016.
[22] M. Gehl, D. Trotter, A. Starbuck, A. Pomerene, A.L. Lentine, and C. DeRose, "High resolution silicon arrayed waveguide gratings for photonic signal processing applications," 2017 Conference on Lasers and Electro-Optics (CLEO), San Jose, CA, USA, May 2017.
[23] A.E. Willner, A. Fallahpour, F. Alishahi, and Y. Cao, "All-optical signal processing techniques for flexible networks," J. Lightwave Technol., vol.37, no.1, pp.21–35, Jan. 2019.

Yuta Kaihori received the B.E. degrees in applied physics in 2019 from Osaka University, Osaka, Japan, where he is currently working toward the M.S. degree in material and life science. His research interest includes optical signal processing.

Yu Yamasaki received the B.E. degrees in applied physics and M.E. degrees in material and life science, in 2016 and 2018, respectively, from Osaka University, Osaka, Japan, where he is currently working toward the Ph.D. degree in advanced science and biotechnology. His research interest includes optical signal processing.

Tsuyoshi Konishi received the B.E., M.E., and Dr.E. degrees in applied physics from Osaka University, Osaka, Japan, in 1991, 1993, and 1995, respectively. Since 1996, he has been with the Graduate School of Engineering (GSE), Osaka University, earlier as an Assistant Professor, and currently, as an Associate Professor in the Division of Advanced Science and Biotechnology. His current research interests include ultrafast optical signal processing. Dr. Konishi is a member of the Institute of Electronics, Information, and Communication Engineers, the Japan Society of Applied Physics, the Optical Society of Japan (OSJ), the Optical Society of America (OSA), and the International Society for Optical Engineering (SPIE).